RAPID REPORT

Induced sharp wave-ripple complexes in the absence of synaptic inhibition in mouse hippocampal slices

Volker Nimmrich[1], Nikolaus Maier[2], Dietmar Schmitz[2] and Andreas Draguhn[3]

[1]*Abbott GmbH & Co. KG, Neuroscience Research, Knollstrasse 50, 67061 Ludwigshafen, Germany*
[2]*Neuroscience Research Centre at the Charité, Charité University Hospital, Schumannstrasse 20/21, 10117 Berlin, Germany*
[3]*Institute of Physiology and Pathophysiology, Heidelberg University, Im Neuenheimer Feld 326, 69120 Heidelberg, Germany*

The characteristic, behaviour-related network oscillations of the mammalian hippocampus (θ, γ and ripples) are accompanied by strongly phase-coupled action potentials in specific subsets of GABAergic interneurones. It has been suggested that the resulting phasic, repetitive inhibition shapes rhythmic coherent activity of the neuronal network. Here, we examined whether synaptic inhibition entrains ∼200 Hz network ripples by applying the $GABA_A$ receptor antagonist gabazine to CA1 minislices of mouse hippocampus. Gabazine blocked spontaneously occurring sharp wave–ripple (SPW–R) activity. However, local application of KCl to the dendritic layer elicited excitatory sharp waves on which ∼200 Hz ripple oscillations were superimposed with equal temporal properties of native SPW–R. The activity also persisted in the additional presence of blockers of glutamatergic synaptic transmission. In contrast, synchrony was largely abolished after addition of gap junction blockers. Thus, GABAergic transmission appears to be involved in the generation of sharp waves but phasic inhibition is no prerequisite for the precise synchronization of hippocampal neurones during high-frequency oscillations at ∼200 Hz. Gap junctions on the other hand seem to be necessary to orchestrate coordinated activity within the ripple frequency domain.

(Resubmitted 19 November 2004; accepted after revision 14 January 2005; first published online 20 January 2005)
Corresponding author A. Draguhn: Institute of Physiology and Pathophysiology, Heidelberg University, Im Neuenheimer Feld 326, 69120 Heidelberg, Germany. Email: andreas.draguhn@urz.uni-heidelberg.de

The mammalian hippocampus displays EEG oscillations at various frequencies related to different behavioural states. Theta (∼5–10 Hz) and gamma band (∼30–80 Hz) activities occur during spatial exploration and rapid eye movement (REM) sleep. At rest and during slow-wave sleep, sharp waves (SPW) and superimposed high-frequency ripples at ∼200 Hz can be observed (O'Keefe & Nadel, 1978; Buzsáki *et al.* 1992). Theta and gamma periods have been implicated in the acquisition of memory contents while sharp wave–ripple complexes (SPW–R) may serve a role in the consolidation of recently acquired memories (Buzsáki, 1998; Siapas & Wilson, 1998). This hypothesis is based on the observation that sequential activation patterns of place cells are established during spatial exploration (O'Keefe & Recce, 1993) and re-played, at faster pace, during SPW–R in subsequent episodes of non-REM sleep (Wilson & McNaughton, 1994; Lee & Wilson, 2002).

Recent work has demonstrated that basket cells and bistratified cells, specific subtypes of inhibitory interneurones, fire strongly phase-coupled action potentials during SPW–R (Klausberger *et al.* 2003, 2004). Such experimental findings, together with computer modelling, have led to the general notion that inhibitory interneurones can entrain multiple target cells into a common, rhythmic activity pattern (Cobb *et al.* 1995; Wang & Buzsáki, 1996; Tamás *et al.* 2000; for review see Whittington & Traub, 2003), although this notion may not apply to all forms of fast hippocampal network oscillations (Bracci *et al.* 1999). In line with this hypothesis, the precise spike timing of pyramidal cells during ripples has been suggested to result from fast, phasic inhibition (Buzsáki *et al.* 1992; Ylinen *et al.* 1995; Klausberger *et al.* 2003).

Here, we have tested this interneurone-network hypothesis for ∼200 Hz ripples. We made use of a recently developed *in vitro* model of SPW–R where this pattern of activity can be recorded in mouse hippocampal slices (Maier *et al.* 2002, 2003). We found that block of $GABA_A$ receptor-mediated synaptic transmission abolishes the

V. Nimmrich and N. Maier contributed equally to this work.

DOI: 10.1113/jphysiol.2004.079558

spontaneous generation of SPW–R but that synchronous field ripples at ∼200 Hz can be reliably restored by dendritic puffs of KCl. Thus, fast synaptic inhibition is no prerequisite for coherent high-frequency network oscillations in the hippocampus.

Methods

Electrophysiology

Experiments were performed on C57Bl/6 mice of both sexes aged 4–8 weeks and were approved by the Berlin state government (T 0386/98). Mice were anaesthetized with ether and decapitated, and the brain was removed. Brains were kept in cooled (∼1–4°C) artificial cerebrospinal fluid (ACSF), containing (mM): NaCl 129, KCl 3, $MgSO_4$ 1.8, $CaCl_2$ 1.6, glucose 10, NaH_2PO_4 1.25, $NaHCO_3$ 21, gassed with 95% O_2–5% CO_2 (pH 7.4 at 37°C). After removal of the cerebellum, horizontal slices of 450 μm were cut on a vibratome (Campden Instruments, Sileby, UK). Minislices of the CA1 region were prepared by isolating area CA1 from the adjacent CA3 and subiculum (see Fig. 1*A*).

Recordings were performed at 35 ± 0.5°C in a modified Haas-type interface chamber and SPW–R could be recorded after 1–2 h of equilibration in the recording

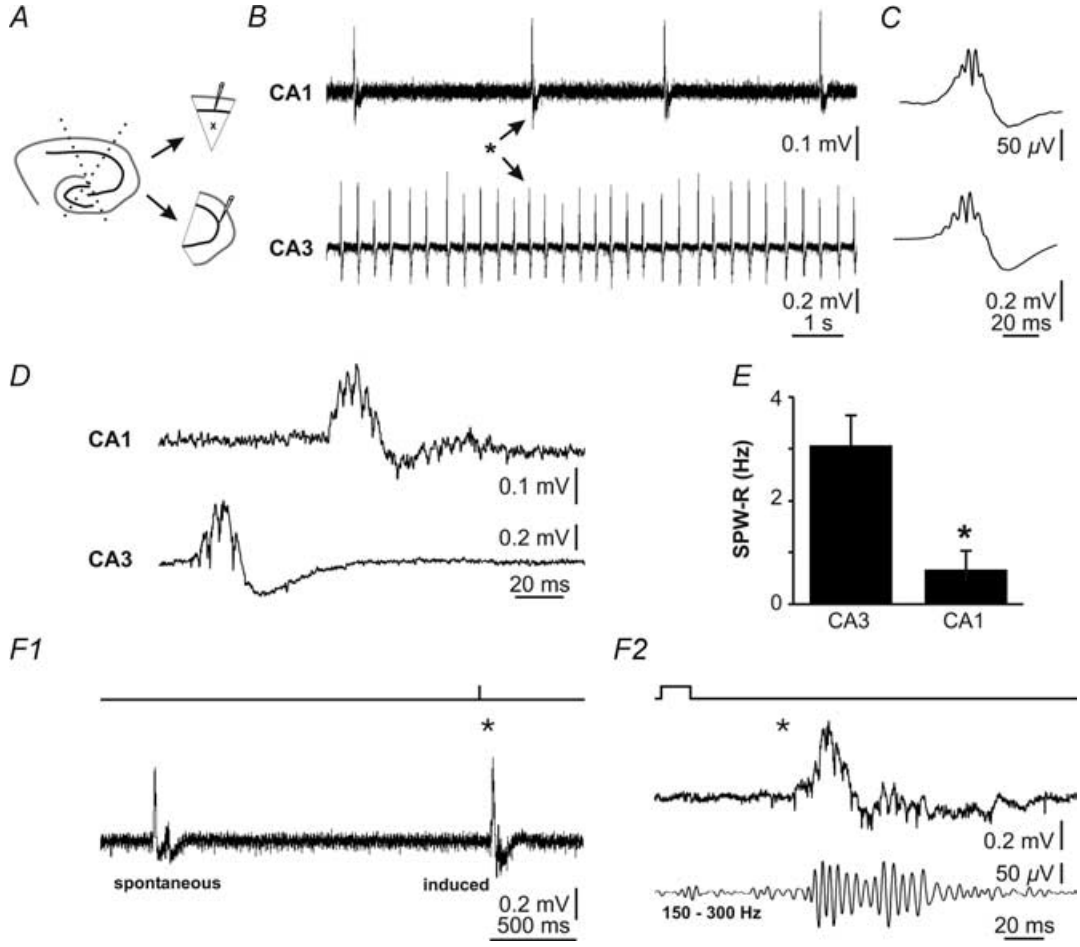

Figure 1. Spontaneous and induced sharp wave–ripple complexes in CA1 minislices
A, schematic illustration of CA1 minislice and the approximate extracellular recording and application (x) pipette positions. *B*, parallel recording from a CA1 minislice and its corresponding remnant CA3 region showing that SPW–R can as well be generated independently in area CA1, though less frequently. *C*, averages from 20 min of spontaneous SPW–R activity in a CA1 minislice (upper panel) and in CA3 (below) from the experiment shown in *B*. Note the similarity of waveforms recorded from CA1 minislice and CA3 remnant. *D*, raw data examples from the events marked in *B*. There is no apparent difference in the appearance of events recorded from a CA1 minislice and its CA3 remnant. *E*, spontaneous SPW–R in CA1 minislices occur five times less frequently as compared to CA3 ($P < 0.05$; six slices from four animals). *F1*, spontaneous and induced SPW–R recorded from CA1 minislice in normal extracellular medium (ACSF). *F2*, induced event from *F1* at higher temporal resolution (upper trace). Below: band pass-filtered derivative isolates SPW associating ∼200 Hz ripples. Square pulse marker (top) gives time and duration of KCl puff.

chamber. Extracellular glass microelectrodes had tip diameters of 5–10 μm and were filled with ACSF before use. For paired intra- and extracellular recordings we used platinum wire electrodes (20 μm diameter) in order to minimize cross-talk between electrodes. Whole-cell recordings of stimulation-induced inhibitory postsynaptic currents were performed using the Multiclamp 700A amplifier (Axon Instruments, Union City, CA, USA). Borosilicate glass electrodes (Harvard Apparatus Ltd, Edenbridge, UK; 2–5 MΩ) were filled with 120 mM caesium gluconate, 5 mM CsCl, 10 mM TEA-Cl, 8 mM NaCl, 10 mM Hepes, 5 mM EGTA, 4 mM MgATP, 0.3 mM Na_3GTP and 5 mM QX-314; pH adjusted to 7.3 with CsOH. Access resistance was not allowed to vary more than 15% during the course of the experiment. No series resistance compensation was used. Sharp microelectrode recordings were performed with a bridge balance amplifier (BA-1S; npi electronics, Tamm, Germany). Electrode (o.d. 1.2 mm) resistance was > 80 MΩ, input resistance of pyramidal cells varied from 40 to 60 MΩ. After impaling a cell, negative current was injected for several minutes until the membrane potential had stabilized and current injection could be gradually reduced to zero. Bridge balance was repeatedly adjusted during the experiment by optimizing the voltage response to small negative current injections (100–200 pA). Intrinsic properties of cells were initially assessed by negative and positive current injections of 200 ms duration. Offset potentials were determined at the end of experiment and were subtracted from the recorded values.

Pressure application of KCl (1 M in ACSF) was performed through a micropipette (tip diameter 5–10 μm) positioned in the dendritic region of area CA1. Pressure parameters were 0.4–2.0 bar, pulse duration 5–30 ms using a custom-made pressure application device or a Picospritzer III (Parker Instrumentation, Chicago, IL, USA). In some control experiments, ACSF was used instead of KCl. Drugs were added from aqueous stock solutions ($\times$ 1000) except 6-cyano-7-nitroquinoxaline-2,3-dione (CNQX; dissolved at 1000-fold in DMSO) and 1-octanol, which we applied directly to ACSF. All drugs were from Sigma/RBI.

Data processing and analysis

Details of data processing and analysis methods were similar to procedures described recently (Maier *et al.* 2003). Briefly, original extracellular data were filtered at 1–3 kHz, sampled at 5–10 kHz with a CED Micro1401 interface (CED, Cambridge, UK) and analysed off-line using the Spike2 software (CED). For detection of ripple oscillations, raw data were band-pass filtered at 150–300 Hz and detection threshold was set at four times the standard deviation of event-free baseline noise or was determined arbitrarily and controlled by visual inspection.

Based on threshold detection algorithms, event markers were set for each ripple trough in band-pass filtered data. We then constructed interspike interval histograms from these events providing a reliable measure of the frequency content of the network oscillations.

Additionally, leading frequency of ripples was determined by the first positive side peak of auto-correlation functions derived from 50 ms raw data epochs. Power spectra (FFT, resolution 20 Hz) were computed from 150 ms data stretches where oscillation amplitudes were maximal. For comparison of different power spectra we calculated the area under the peak by integrating over the ripple frequency band (120–250 Hz).

Quantitative results are given as means ± S.D. Groups of paired data were compared using the non-parametric Wilcoxon's test with $P < 0.05$ regarded as significant.

Results

In extracellular field potential recordings from stratum pyramidale of CA1 minislices we regularly observed spontaneously occurring sharp wave–ripple complexes (SPW–R; Fig. 1). However, the frequency of occurrence of SPW–R in these minislices was clearly lower than in the dissected corresponding CA3 region (0.7 ± 0.4 Hz *versus* 3.1 ± 0.6 Hz; 6 slices out of 4 animals; $P < 0.05$; Fig. 1*B* and *E*). The morphology of such SPW–R could not be distinguished from similar events in intact hippocampal slices (Fig. 1*B–D*) indicating that this pattern of activity can be generated within the local network of CA1. Field events could also be elicited by local pressure-application of KCl (1 M) into the dendritic field of CA1. When duration and pressure of KCl puffs were appropriately tuned, these transient field potential responses in stratum pyramidale resembled spontaneous SPW–R (see Fig. 1*F*). Pressure-application of ACSF never induced any significant field potential response ($n = 15$ slices).

In order to elucidate the role of GABAergic inhibition for the organization of SPW–R we added the $GABA_A$ receptor antagonist SR95531 (gabazine) to the bath solution. As expected, epileptiform activity was absent in CA1 minislices, which was the rationale for using this preparation. In the corresponding CA3 remnants, interictal-like discharges were regularly observed (7/9 slices showing epileptiform discharges; Fig. 3*A*). The effect of gabazine was quantified by whole-cell recordings of stimulus-evoked inhibitory postsynaptic currents in CA1 pyramidal cells in the presence of glutamate receptor blockers (20 μM CNQX; 30 μM D-APV). Evoked IPSCs were reduced to $33.1 \pm 10.4\%$ of control at 0.3 μM gabazine ($n = 7$) and were virtually abolished at 1.0 μM

(4.8 ± 3.3%; $n = 4$; Fig. 2*D–F*). At 1 μM, gabazine rapidly and completely suppressed the spontaneous generation of SPW–R in CA1 minislices (see Fig. 3*A1*). At 0.3 μM, however, the block developed more slowly (Fig. 2*A* and *C*), enabling a detailed analysis of SPW–R during the transition phase from partial to full block. We analysed spontaneous SPW–R at a time when the activity was suppressed by ∼80%. The remaining events displayed normal waveform (Fig. 2*B*) and our recordings did contain discernible ripple oscillations at similar frequency of occurrence as under control conditions ($P > 0.05$; $n = 5$ slices; Fig. 2*C*). These results indicate that $GABA_A$ receptors are involved in the generation of SPW–R but that full synaptic inhibition is not needed for the organization of ∼200 Hz ripples within the local CA1 network.

To further test for this hypothesis, we evoked sharp waves by dendritic potassium puffs (focal application of 1 M KCl, 5–30 ms) in the presence of gabazine (0.3 μM, 1.0 μM and 10 μM, respectively). The induced field potential waves in stratum pyramidale were regularly superimposed by fast oscillatory activity (Fig. 3). Together, these responses resembled normal SPW–R. A quantitative analysis of interspike intervals confirmed the similarity between spontaneous SPW–R (from five slices) and evoked events in normal ACSF ($n = 96$ events, 12 slices), in 0.3 μM gabazine ($n = 37$ events from seven slices), in 1.0 μM gabazine ($n = 89$ events; five slices), and in 10 μM gabazine ($n = 91$ events; eight slices; Fig. 4*A*). Likewise, analysis of leading frequencies derived from autocorrelation functions of raw data showed no difference between spontaneous and evoked SPW–R in the absence or presence of 10 μM gabazine (Fig. 4*C*). In order to test whether $GABA_A$ receptor-mediated signalling was entirely suppressed by 1 or 10 μM gabazine

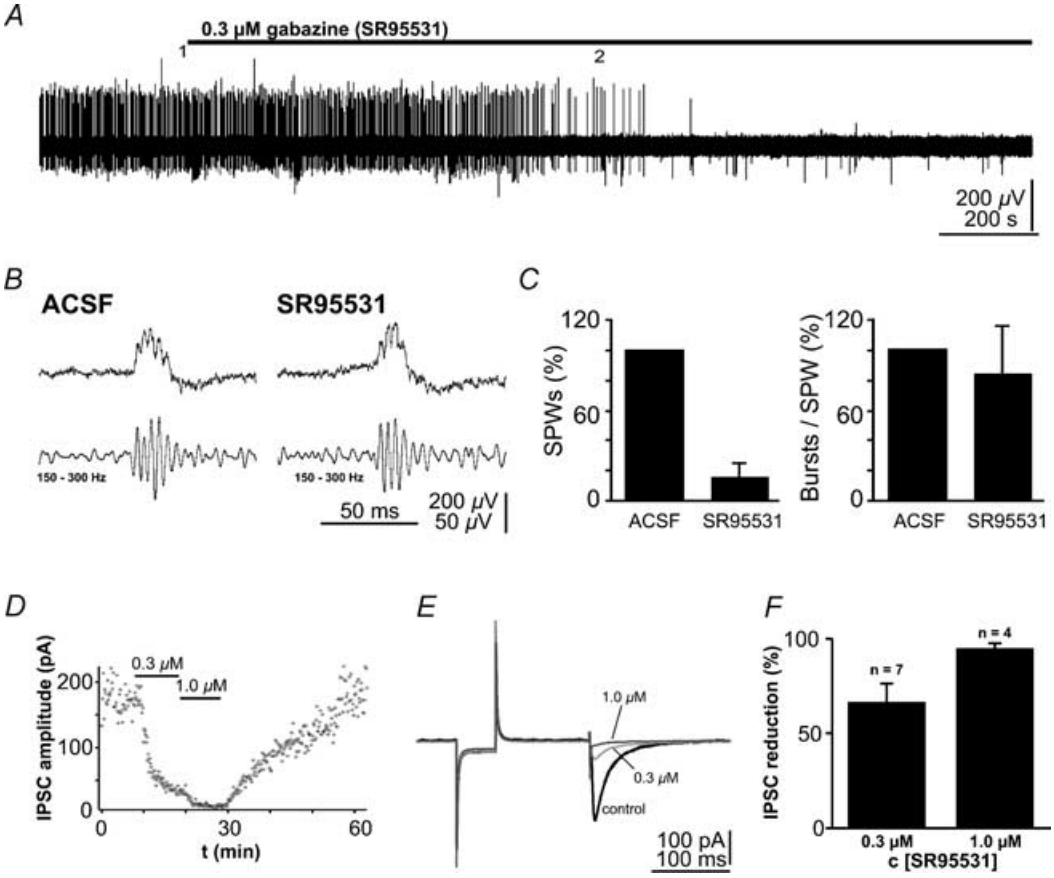

Figure 2. Action of gabazine on spontaneous SPW–R and induced IPSCs
A, spontaneously occurring SPW–R are suppressed by 0.3 μM gabazine. *B*, events recorded before application of SR95531 (left, marked 1 in *A*) and remaining SPW–R during transition phase (right, marked 2 in *A*) show identical shape of waveforms. *C*, left: suppression of spontaneous SPW–R activity by 0.3 μM gabazine at the time of analysis ($n = 5$); within the same time windows number of ripple bursts per sharp wave did not change in the remaining events (right). *D*, time course of gabazine action in a CA1 pyramidal cell showing reversible suppression of stimulus-induced IPSCs. *E*, superimposed data traces from the experiment shown in *D*. Traces are averaged over 10 original data sweeps (stimulus artefact truncated). *F*, IPSC amplitude reduction at different gabazine concentrations (group data). Stimulus-evoked IPSCs were reduced by 66.9 ± 10.4% at 0.3 μM ($n = 7$) and 95.2 ± 3.3% at 1.0 μM gabazine ($n = 4$).

during KCl-evoked activity we recorded intracellularly from five putative pyramidal cells. Evoked field events were regularly accompanied by depolarizing intracellular potentials with or without superimposed spikes (Fig. 3*B*). Depolarization of the cells up to –45 mV did not reveal any hyperpolarizing component, largely excluding inhibitory synaptic signalling. If $GABA_A$ receptor activation is not required to coordinate network activity at ∼200 Hz, other fast signalling mechanisms must be involved. We therefore added glutamate receptor blockers on top of 10 μM gabazine. Surprisingly, this treatment also did not alter the KCl-induced ripples (Fig. 4*B*, *C* and *D1*). Finally, we suppressed electrical coupling by gap junctions, in addition to the receptor blockers. Octanol (1 mM) largely abolished the regular autocorrelation of KCl-induced events (Fig. 4*D*) and reduced the power of the ripple-band (120–250 Hz) by 60% compared to control ($n = 6$, $P < 0.05$). Similar results were obtained with carbenoxolone (200 μM, $n = 4$; data not shown).

Discussion

Inhibitory interneurones are considered key regulatory elements in the synchronization of oscillating cortical neuronal assemblies (Whittington & Traub, 2003). Ripples, a particularly fast network oscillation, are accompanied by fast series of Cl^--dependent IPSPs in pyramidal cells (Ylinen *et al.* 1995; Buzsáki *et al.* 1996), consistent with the fast kinetics of synaptic inhibition at hippocampal pyramidal cells (Bartos *et al.* 2002).

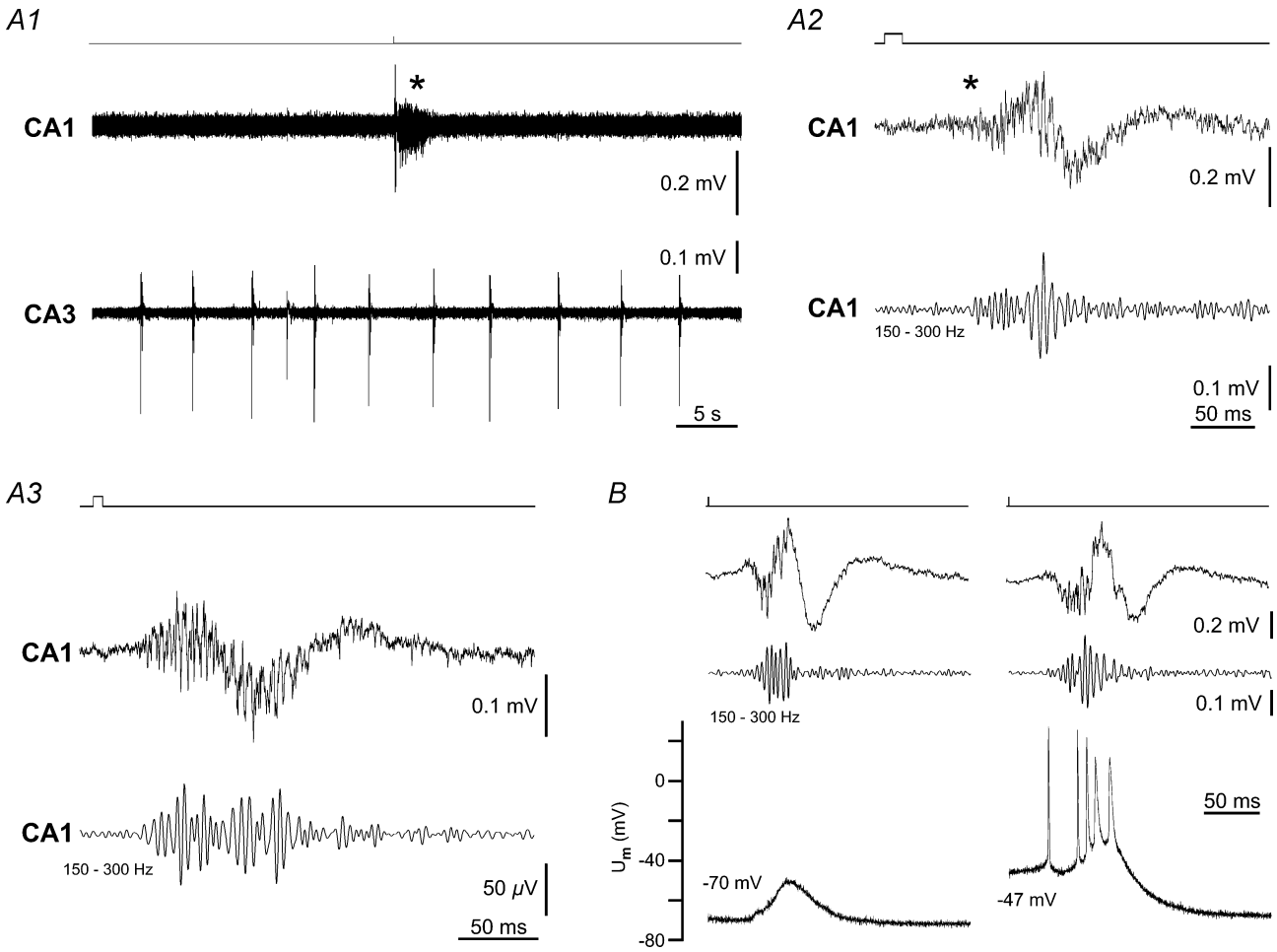

Figure 3. Reconstitution of sharp wave-ripple complexes in the absence of fast synaptic inhibition
A1, puff application of KCl (1 M) into stratum radiatum of CA1 minislice in the presence of 1 μM gabazine (upper trace). Note that there is no spontaneous activity within CA1 in contrast to epileptiform discharges in the respective CA3 remnant (bottom trace). Top: square pulse marker corresponds to time and duration of KCl puff. *A2*, higher temporal resolution of the reconstituted SPW–R shown in *A*. Bottom trace gives the band pass filtered derivative showing the isolated ripple burst. *A3*, KCl puff-induced event at 10 μM gabazine (upper trace) and band pass filtered high-frequency ripple (bottom). *B*, paired extra- (top) and intracellular (bottom trace) recordings from a putative pyramidal cell at 1 μM gabazine at two different membrane potentials (stimulation parameters constant during experiment). At both membrane potentials, SPW–R are accompanied by transient depolarizing potentials without apparent phasic inhibitory postsynaptic potentials.

Moreover, certain interneurones fire phase-synchronized fast series of action potentials during ripples (Csicsvari *et al.* 1999; Klausberger *et al.* 2003, 2004). These observations have led to the suggestion that phasic inhibition plays a causal role in the temporal organization of ripple network activity (Buzsáki *et al.* 1992; Ylinen *et al.* 1995; Klausberger *et al.* 2003). Our present data show that inhibitory postsynaptic potentials are not

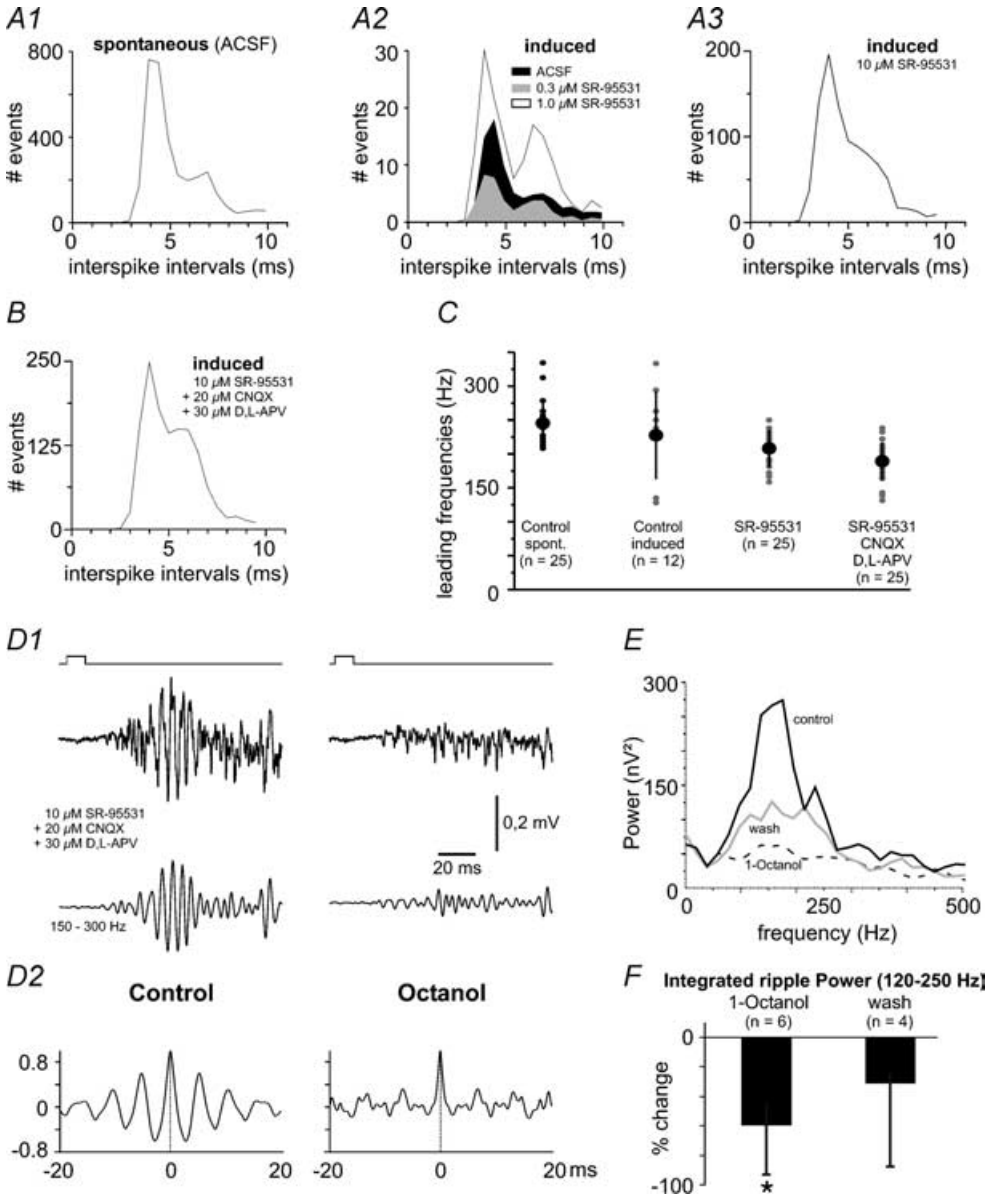

Figure 4. Mechanisms of synchrony during ripples
A1–3, cumulative interspike interval histograms of reconstituted events and ripples from control conditions. Note corresponding peaks at 4–5 ms at different experimental conditions: spontaneous sharp wave-associated ripples (*A1*, 5 slices) and induced events in ACSF (*A2*, black histogram, $n = 96$ events from 12 slices); at 0.3 μM and 1.0 μM (*A2*, $n = 37$ events, 7 slices and $n = 89$ events, 5 slices; grey and white histograms, respectively) and 10 μM gabazine ($n = 91$ events, 8 slices; *A3*). *B*, cumulative interspike interval histogram from events recorded in 10 μM gabazine, 20 μM CNQX and 30 μM ±-APV ($n = 100$ events, 10 slices). *C*, leading frequencies derived from first positive side peaks of autocorrelation functions of single KCl-induced events. Numbers of respective events analysed and experimental conditions as mentioned. No significant change by blockers of GABAergic or glutamatergic transmission. *D1*, example of evoked events in the combined presence of $GABA_A$ receptor- and glutamate receptor antagonists (control, left) and after additional block of gap junctions by 1 mM 1-octanol (right). Note loss of network oscillation and network synchrony under octanol (*D2*). *E*, power spectra of 10 consecutive KCl-induced events (150 ms each) from control slices (10 μM gabazine, 20 μM CNQX, and 30 μM ±-APV) and after > 40 min of application of 1-octanol. Note reduction of ripple frequency power under the action of the gap junction blocker. *F*, group data. In six experiments, ripple power (integrated over 120–250 Hz) was reduced by 60% compared to control ($P < 0.05$), which was partially reversible.

needed to synchronize neuronal assemblies at ∼200 Hz. In contrast, $GABA_A$ receptor-mediated transmission seems to be involved in the initiation of SPW–R, acting as a trigger for the compound network depolarizing potentials rather than organizing the neuronal discharges within SPW–R. The mechanisms underlying this counter-intuitive role of $GABA_A$ receptor-mediated action have not been clarified but may involve synchronized discharges of electrically coupled interneurones or rebound activation of pyramidal cells (see, for discussion, Maier *et al.* 2002).

In hippocampal slices from rats, ∼200 Hz network activity can be elicited in calcium-free solutions where chemical synaptic transmission is blocked (Draguhn *et al.* 1998). These events do not, however, resemble native SPW–R as closely as spontaneous network activity in slices from mice (Maier *et al.* 2002, 2003). In the mouse preparation we have already shown that SPW–R depend on excitatory synaptic transmission as well as on electrical coupling (Maier *et al.* 2003), in line with accompanying theoretical work (Traub *et al.* 1999). Our present findings show that excitatory transmission can be replaced by K^+-driven dendritic depolarizations and is not needed for synchronization of ∼200 Hz network oscillations. Using blockers of electrotonic coupling, we further confirmed the crucial role of gap junctions for network synchrony at this frequency (see also Traub *et al.* 1999; Traub & Bibbig, 2000; Whittington & Traub, 2003). It must be noted, however, that the pharmacological agents affecting gap junctions are poorly selective and may even fail to block electrical coupling under some conditions (Rouach *et al.* 2003). The role of synaptic inhibition for ripples is even less clear. Models and experimental work indicate that $GABA_A$ receptor-mediated transmission can stabilize fast oscillatory activity and determine its frequency (Traub & Bibbig, 2000; Traub *et al.* 2003). However, the dependence of SPW–R activity on GABAergic transmission is difficult to test directly because blocking this function induces epileptiform activity in brain slices (Maier *et al.* 2003). Such hyper-synchronous activity can mask more subtle network events like normal SPW–R. Here we made use of the CA1 minislice preparation, which does not display epileptiform activity upon disinhibition, possibly due to the low number of recurrent excitatory collaterals (Deuchars & Thomson, 1996). In contrast to recent observations in rat hippocampal slices (Colgin *et al.* 2004) spontaneous SPW–R were present in mouse CA1 minislices, albeit at lower frequency. Using this preparation we show that fast IPSPs are not a crucial part of SPW–R.

If synaptic inhibition is not needed to generate synchronized activity at ripple frequency, what could be its functional role during normal SPW–R? It has been noted that only a minority of pyramidal cells are active during SPW–R (Buzsáki *et al.* 1992; Maier *et al.* 2003) while the majority of projection neurones seems to be efficiently inhibited. Considering the finding that ripples re-play specific activation sequences of place cells (Wilson & McNaughton, 1994; Lee & Wilson, 2002) it is feasible that inhibition serves to suppress activity in those pyramidal cells which are not part of the activated assembly. Thereby, synaptic inhibition would enhance signal-to-noise ratio for information transfer in the two-stage memory model of hippocampal function (Buzsáki, 1989; 1998).

References

Bartos M, Vida I, Frotscher M, Meyer A, Monyer H, Geiger JR & Jonas P (2002). Fast synaptic inhibition promotes synchronized gamma oscillations in hippocampal interneuron networks. *Proc Natl Acad Sci U S A* **99**, 13222–13227.

Bracci E, Vreugdenhil M, Hack SP & Jefferys JG (1999). On the synchronizing mechanisms of tetanically induced hippocampal oscillations. *J Neurosci* **19**, 8104–8113.

Buzsáki G (1989). Two-stage model of memory trace formation: a role for 'noisy' brain states. *Neuroscience* **31**, 551–570.

Buzsáki G (1998). Memory consolidation during sleep: a neurophysiological perspective. *J Sleep Res* **7** (Suppl. 1), 17–23.

Buzsáki G, Horváth Z, Urioste R, Hetke J & Wise K (1992). High-frequency network oscillation in the hippocampus. *Science* **256**, 1025–1027.

Buzsáki G, Penttonen M, Nádasdy Z & Bragin A (1996). Pattern and inhibition-dependent invasion of pyramidal cell dendrites by fast spikes in the hippocampus *in vivo*. *Proc Natl Acad Sci U S A* **93**, 9921–9925.

Cobb SR, Buhl EH, Halasy K, Paulsen O & Somogyi P (1995). Synchronization of neuronal activity in hippocampus by individual GABAergic interneurons. *Nature* **378**, 75–78.

Colgin LL, Kubota D, Jia Y, Rex CS & Lynch G (2004). Long-term potentiation is impaired in rat hippcampal slices that produce spontaneous sharp waves. *J Physiol* **558**, 953–961.

Csicsvari J, Hirase H, Czurkó A, Mamiya A & Buzsáki G (1999). Oscillatory coupling of hippocampal pyramidal cells and interneurons in the behaving rat. *J Neurosci* **19**, 274–287.

Deuchars J & Thomson AM (1996). CA1 pyramid-pyramid connections in rat hippocampus *in vitro*: dual intracellular recordings with biocytin filling. *Neuroscience* **74**, 1009–1018.

Draguhn A, Traub RD, Schmitz D & Jefferys JG (1998). Electrical coupling underlies high-frequency oscillations in the hippocampus *in vitro*. *Nature* **394**, 189–192.

Klausberger T, Magill PJ, Marton LF, Roberts JD, Cobden PM, Buzsáki G & Somogyi P (2003). Brain-state- and cell-type-specific firing of hippocampal interneurons *in vivo*. *Nature* **421**, 844–848.

Klausberger T, Marton LF, Baude A, Roberts JD, Magill PJ & Somogyi P (2004). Spike timing of dendrite-targeting bistratified cells during hippocampal network oscillations *in vivo*. *Nat Neurosci* **7**, 41–47.

Lee AK & Wilson MA (2002). Memory of sequential experience in the hippocampus during slow wave sleep. *Neuron* **36**, 1183–1194.

Maier N, Güldenagel M, Söhl G, Siegmund H, Willecke K & Draguhn A (2002). Reduction of high-frequency network oscillations (ripples) and pathological network discharges in hippocampal slices from connexin 36-deficient mice. *J Physiol* **541**, 521–528.

Maier N, Nimmrich V & Draguhn A (2003). Cellular and network mechanisms underlying spontaneous sharp wave-ripple complexes in mouse hippocampal slices. *J Physiol* **550**, 873–887.

O'Keefe J & Nadel L (1978). *The Hippocampus as a Cognitive Map*. Oxford University Press, Oxford.

O'Keefe J & Recce ML (1993). Phase relationship between hippocampal place units and the EEG theta rhythm. *Hippocampus* **3**, 317–330.

Rouach N, Segal M, Koulakoff A, Giaume C & Avignone E (2003). Carbenoxolone blockade of neuronal network activity in culture is not mediated by an action on gap junctions. *J Physiol* **553**, 729–745.

Siapas AG & Wilson MA (1998). Coordinated interactions between hippocampal ripples and cortical spindles during slow-wave sleep. *Neuron* **21**, 1123–1128.

Tamás G, Buhl EH, Lorincz A & Somogyi P (2000). Proximally targeted GABAergic synapses and gap junctions synchronize cortical interneurons. *Nat Neurosci* **3**, 366–371.

Traub RD & Bibbig A (2000). A model of high-frequency ripples in the hippocampus based on synaptic coupling plus axon-axon gap junctions between pyramidal neurons. *J Neurosci* **20**, 2086–2093.

Traub RD, Cunningham MO, Gloveli T, LeBeau FE, Bibbig A, Buhl EH & Whittington MA (2003). GABA-enhanced collective behavior in neuronal axons underlies persistent gamma-frequency oscillations. *Proc Natl Acad Sci U S A* **100**, 11047–11052.

Traub RD, Schmitz D, Jefferys JG & Draguhn A (1999). High-frequency population oscillations are predicted to occur in hippocampal pyramidal neuronal networks interconnected by axoaxonal gap junctions. *Neuroscience* **92**, 407–426.

Wang XJ & Buzsáki G (1996). Gamma oscillation by synaptic inhibition in a hippocampal interneuronal network model. *J Neurosci* **16**, 6402–1643.

Whittington MA & Traub RD (2003). Interneuron diversity series: inhibitory interneurons and network oscillations *in vitro*. *Trends Neurosci* **26**, 676–682.

Wilson MA & McNaughton BL (1994). Reactivation of hippocampal ensemble memories during sleep. *Science* **265**, 676–679.

Ylinen A, Bragin A, Nádasdy Z, Jandó G, Szabó I, Sik A & Buzsáki G (1995). Sharp wave-associated high-frequency oscillation (200 Hz) in the intact hippocampus: network and intracellular mechanisms. *J Neurosci* **15**, 30–46.

Acknowledgments

This work was supported by the Deutsche Forschungsgemeinschaft (DFG Dr 326/ 1-3 to AD and an Emmy-Noether-Grant to DS). We gratefully acknowledge the work of Drs. Hans-Jürgen Gabriel and Herbert Siegmund on data analysis and helpful discussions with Prof. Uwe Heinemann.